JOURNAL OF VIROLOGY, June 1990, p. 2632–2641
0022-538X/90/062632-10$02.00/0

Vol. 64, No. 6

Rotavirus Proteins VP7, NS28, and VP4 Form Oligomeric Structures

DAVID R. MAASS AND PAUL H. ATKINSON*

Department of Developmental Biology and Cancer, Albert Einstein College of Medicine, Bronx, New York 10461

Received 11 October 1989/Accepted 27 February 1990

Sucrose gradient sedimentation analysis of rotavirus SA11-infected Ma104 cells revealed the presence of oligomers of VP7, the structural glycoprotein, and NS28, the nonstructural glycoprotein. Cross-linking the proteins, either before or after sucrose gradient centrifugation, stabilizes oligomers, which can be analyzed by nonreducing sodium dodecyl sulfate-polyacrylamide gel electrophoresis (SDS-PAGE) after immunoprecipitation. The major NS28 oligomer was tetrameric, though dimers and higher-order structures were observed as well. VP7 formed predominantly dimers, and again tetramers and higher oligomeric forms were present. Each oligomer of VP7 and NS28 sedimented at the same characteristic rate through the sucrose gradient either in the presence or absence of cross-linking. Monomers could not be cross-linked to form oligomers, demonstrating that cross-linked oligomers were not artifactually derived from monomers. Reversing the cross-linking of immunoprecipitated VP7 on reducing SDS-PAGE resulted in the appearance of only the monomeric form of VP7. Dissociation of the NS28 oligomers resulted in stable dimers as well an monomers. In the faster-sedimenting fractions, a 16S to 20S complex, which contained the rotavirus outer shell proteins VP7 and VP4 cross-linked to NS28, was observed. These complexes were shown not to be associated with any known subviral particle. The association of VP4, NS28, and VP7 may represent sites on the endoplasmic reticulum membrane that participate in the budding of the single-shelled particles into the lumen of the endoplasmic reticulum, where maturation to double-shelled particles occurs.

Rotavirus, a member of the *Reoviridae* causing intestinal gastroenteritis, buds into the rough endoplasmic reticulum (ER) during maturation (1, 12, 18, 24, 28, 47). In its mature form, like other members of the genus, the virion is a double-shelled proteinaceous particle of icosahedral symmetry. The inner shell, enclosing the 11 segments of double-stranded RNA genome, consists of VP1, VP2, VP3, and the nucleocapsid, VP6 (28, 31). The outer shell is made up of the structural glycoprotein VP7 (16) and the hemagglutinin VP4 (27). VP7 or NS35 is thought to be involved in cell attachment during infection (4, 19, 45). Part of the nonstructural glycoprotein, NS28, functions as a cytoplasmically oriented receptor for single-shelled particles (2, 3, 35).

The two glycoproteins, VP7 and NS28, are restricted to the rough ER (12, 13, 38, 39, 43). NS28 is encoded by genome segment 10 (5, 10, 36) and is a protein of 175 amino acids containing three hydrophobic domains, H1, H2, and H3, near the N terminus (10). It is an integral membrane protein (17, 25) and is thought to have at least one membrane-spanning domain (7, 11). H1 has two N-linked glycosylation sites at residues 8 and 18 (10) which contain high-mannose carbohydrates of the $Man_8GlcNAc$ and $Man_9GlcNAc$ species (25) and thus is luminally oriented. H2 is the internal uncleaved signal and membrane anchor sequence (7). H3, in vitro, is protected from proteases in microsomes even though it is on the exterior of microsomes (7, 11), suggesting the presence of secondary or tertiary structure resistant to proteases. Computer hydrophobic moment plot analysis suggested that H2 was a multimeric transmembrane region (11).

VP7, encoded by genome segment 9 (9, 21, 42), is a membrane-associated protein (25). The open reading frame codes for 326 amino acids containing two hydrophobic domains of amino acids near the N terminus, each preceded by a methionine (9). In vitro translation and transfection studies have shown that the first hydrophobic domain is not necessary for insertion into the ER and in most cases is probably not translated (41). The second hydrophobic domain is translated and is cleaved, resulting in glutamine 51 at the mature N terminus (50). It has been reported that this membrane translocation signal may be involved in the retention of VP7 in the ER (49). Sequences near the mature N terminus were also shown to be necessary for retention of VP7 in the ER (40, 41), although the mechanism of retention remains unclear.

It has been well documented that other viral membrane glycoproteins need to fold and oligomerize properly before transport from the ER to the Golgi apparatus can occur (14, 15, 20, 29, 44). Thus, it was of interest to investigate whether the membrane glycoproteins encoded by rotavirus could also form multimeric structures even though the rotavirus glycoproteins do not normally exit the ER via the secretory pathway.

As the virus matures, it transiently acquires a membrane envelope that is subsequently removed, and the outer shell proteins, VP7 and VP4, are assembled onto the single-shelled particle to form the double-shelled particle (1, 13, 18, 24, 28, 47). VP7 is restricted to the lumen of the ER (13, 38, 39), whereas VP4 is thought to be located in the cytoplasm, possibly between the ER and the viroplasm (26, 39). The mechanism by which these two proteins that are located on opposite sides of a membrane associate in a precise fashion to form a double-shelled particle is unknown.

We demonstrate that the rotavirus glycoproteins form oligomers and that VP7, NS28, and VP4 can form a heteroligomer, which we propose may be of significance to the viral assembly process.

MATERIALS AND METHODS

Cells and virus. The fetal rhesus monkey kidney cell line Ma104 and Cos-7 cells (23) were grown as a monolayer in

* Corresponding author.

Dulbecco modified Eagle medium (DMEM) at 37°C. The growth medium was supplemented with 5% fetal bovine serum, 5% calf serum, 2 mM L-glutamine, 100 U of penicillin per ml, and 100 μg of streptomycin per ml (all from GIBCO Laboratories, Grand Island, N.Y.). Simian rotavirus SA11 was propagated at low multiplicity of infection and purified by the procedure of Street et al. (51). Antisera used were (i) L56, rabbit polyclonal antiserum, raised against denatured SA11 VP7 purified from a sodium dodecyl sulfate (SDS)-polyacrylamide gel (41), (ii) 72A4, a monoclonal antiserum directed against the viral particle form of VP7 (26; provided by A. R. Bellamy, Department of Cellular and Molecular Biology, University of Auckland, Auckland, New Zealand), and (iii) anti-NS28, a rabbit polyclonal antiserum raised against a gel-purified NS28–β-galactosidase fusion protein (7; provided by J. Rothblatt, Department of Biochemistry, University of California, Berkeley).

Radiolabeling of rotavirus-infected cells. Confluent monolayers of Ma104 cells in 100-mm-diameter petri dishes were infected with 30 PFU of trypsin-activated rotavirus per cell as described elsewhere (16). At 5.5 h postinfection, the medium was changed to methionine-deficient DMEM (4.0 ml per dish) buffered to pH 7.4 with 10 mM (3-*N*-morpholino) propanesulfonic acid (MOPS)–10 mM *N*-tris(hydroxymethyl)methyl-2-aminoethanesulfonic acid (TES)–15 mM *N*-2-hydroxyethylpiperazine-*N'*-2-ethanesulfonic acid (HEPES) (Research Organics Inc., Cleveland, Ohio) and containing 3 μg of dactinomycin (Calbiochem-Behring, La Jolla, Calif.) per ml. After 10 min, the cells were labeled for 60 min with 1 ml of methionine-deficient buffered DMEM containing 100 μCi of L-[^{35}S]methionine (800 to 1,200 Ci/mmol; Amersham Corp., Arlington Heights, Ill.) and 3 μg of dactinomycin per ml on a rocking platform. The infected cells were rinsed and harvested in ice-cold phosphate-buffered saline (PBS) by scraping with a rubber policeman.

Sucrose gradient sedimentation. Triton X-100-solubilized infected cell lysates (100-mm-diameter plate) were prepared by adding 200 μl of 1.0% Triton X-100, 150 mM NaCl, 50 mM Tris hydrochloride (pH 7.5), and 2 mM phenylmethylsulfonyl fluoride to the pelleted cells. This suspension was vortexed for 30 s and spun in a microfuge for 5 min at 4°C. The supernatants were layered onto 5 to 20% (wt/wt) linear sucrose gradients in 100 mM NaCl–20 mM Tris (pH 7.5)–30 mM MOPS (pH 7.5)–0.1% Triton X-100. Thus, all sucrose gradient sedimentation analyses were performed on lysates in the nondenatured state. The gradients were centrifuged in an SW40 rotor at 37,000 rpm (175,000 × *g*) at 4°C. The runs were terminated at $\omega^2 t$ ranging from 0.6×10^{12} to 1.9×10^{12} rads^2/s. Fractions of 200 μl were collected by puncturing the bottom of the tube and collecting 20 drops. Fractions were pooled in groups of four with neighboring fractions; 1/10 of each subsequent fraction was removed for polyacrylamide gel electrophoresis (PAGE), and the remainder was immunoprecipitated. Sucrose gradients were also overlayed with 0.25 and 0.10 volumes of cell lysate as a control for overloading of the gradients; these gradients showed the same sedimentation profile of infected intracellular proteins as the experimental gradients. $s_{20,w}$ values were determined by use of tables by McEwen (34); standards used (all from Sigma Chemical Co., St. Louis, Mo.) were cytochrome *c* (12,400 daltons [Da]; 1.9S), carbonic anhydrase (29,000 Da; 3.06S), ovalbumin (45,000 Da; 3.7S), bovine serum albumin (66,000 Da; 5.1S), hexokinase (100,000 Da; 5.8S), yeast alcohol dehydrogenase (150,000 Da; 7.6S), and catalase (250,000 Da; 11.3S), which were run in parallel tubes.

Cross-linking. Chemical cross-linking was performed by using the cleavable homobifunctional cross-linker dithiobis (succinimidylpropionate) (DSP; Pierce Chemical Co., Rockford, Ill.). A freshly made 50-mg/ml solution in dimethyl sulfoxide was added to Triton X-100-solubilized infected cell lysates (prepared as described above) to a final concentration of 2% dimethyl sulfoxide (1 mg of DSP per ml) and incubated at 25°C for 60 min. The reaction was terminated by the addition of 2 mM glycine, and the sample was analyzed by sucrose velocity sedimentation. In addition, pooled fractions obtained after sucrose velocity sedimentation as described above were cross-linked by the same procedure. Cross-linked complexes were cleaved by the addition of 50 mM dithiothreitol (DTT).

For cross-linking studies in cells whose membranes were not solubilized, semi-intact cells were prepared as described previously (6). Infected monolayers were washed on the plate twice with 90 mM KCl–50 mM HEPES (pH 7.5) and then three times with 15 mM KCl–10 mM HEPES (pH 7.5). The cells were allowed to swell by incubation with 15 mM KCl–10 mM HEPES (pH 7.5) on ice and then scraped with a rubber policeman into 1.5 ml of 90 mM KCl–50 mM HEPES (pH 7.5). Cells were pelleted at 2,000 rpm for 5 min at 4°C and suspended in 400 μl of 1× PBS, and a sample was tested for trypan blue exclusion. Greater than 90% of the cells were able to take up trypan blue. Either DSP was added as described above or its water-soluble analog 3,3'-dithiobis (sulfosuccinimidylpropionate) (DTSSP; Pierce) was added to cells at 1 mg/ml and allowed to react for 60 min at 25°C, at which time 2 mM glycine was added to terminate the reaction. The cells were then solubilized by the addition of 22 μl of 20% Triton X-100 and spun down in a microfuge for 10 min at 4°C. The supernatant was then immunoprecipitated under denaturing conditions as described below.

Immunoprecipitation. Sucrose gradient fractions of lysates sedimented in the nondenatured state and Triton X-100-solubilized cell lysates were immunoprecipitated with antigens in the denatured state (boiled in SDS) or the nondenatured state (dissolved in Triton X-100) as previously described (8, 41). It was necessary to use denatured antigens in most cases, since available antisera were raised against denatured antigens. Immunoprecipitation of sucrose fractions under denaturing conditions was achieved by adding 20% SDS to a final concentration of 1% and boiling for 4 min. This step was omitted for immunoprecipitation under nondenaturing conditions. Denatured cell lysates were prepared by addition of 150 μl of lysis buffer (1% Triton X-100, 1% deoxycholate [DOC], 0.15 M NaCl, 0.025 M Tris hydrochloride [pH 8.0], 0.1% SDS, 100 U of aprotinin per ml) to the pelleted cells, which were then vortexed for 30 s before addition of 50 μl of 2% DOC–2% Nonidet P-40 in 1× PBS. The cells were again vortexed and spun in an Eppendorf microfuge for 10 min at 4°C to obtain a postnuclear solubilized lysate. This supernatant was transferred to a new Eppendorf tube, 22 μl of 20% SDS was added, the mixture was boiled for 4 min. Samples containing denatured antigens had added 1.0 ml of buffer A (0.19 M NaCl, 0.05 M Tris hydrochloride [pH 7.4], 0.005 M EDTA, 2.5% Triton X-100, 1 mg of bovine serum albumin per ml, 0.001 M L-methionine, 100 U per of aprotinin per ml) and 37 μl of 16.6% Triton X-100. Samples containing nondenatured antigens had added an equal volume of 1% Nonidet P-40–0.15 M NaCl–0.05 M Tris (pH 7.5)–2 mM glucose–4 mM phenylmethylsulfonyl fluoride. To either the denatured or nondenatured supernatants, 2 to 5 μl of the desired antibody (hyperimmune serum) was added to the lysates. In addition, 5 μl of a mixture of affinity-purified goat anti-rabbit immunoglobulin A (IgA),

IgG, and IgM (Organon Teknika, Malvern, Pa.) was added for immunoprecipitations with the monoclonal antibody 72A4 to make the latter bind to the protein-A Sepharose CL4B beads (Pharmacia, Inc., Piscataway, N.J.). Samples were allowed to incubate at 4°C on a rocking platform (Nutator; Clay Adams, Parsippany, N.J.) for 4 to 16 h, followed by addition of 2 mg of protein-A Sepharose CL4B beads and a further 2-h incubation on the Nutator; then the beads were pelleted. For samples containing denatured antigens, the beads were washed three times with buffer B (0.15 M NaCl, 0.01 M Tris hydrochloride [pH 8.3], 0.1% Triton X-100, 0.005 M EDTA, 100 U of aprotinin per ml) and once with 1× PBS. For samples containing nondenatured antigens, the beads were washed three times with 1% Nonidet P-40–0.5% DOC–0.1% SDS–0.5 M NaCl–0.05 M Tris hydrochloride (pH 7.5) and once with 1× PBS. The protein-antibody conjugate was dissociated from the protein A by boiling for 4 min in 1% SDS–50 mM Tris (pH 6.7). The solution was buffered to pH 5.5 by the addition of 0.2 M citrate phosphate (pH 5.0), 2.2 mU of endo-β-*N*-acetylglucosaminidase H (endo H; a gift from R. Trimble, New York State Department of Health, Albany) was added, and the solution was incubated at 37°C for 45 min. The reaction was terminated by the addition of an equal volume of 200 mM Tris–0.64% SDS–2 mM EDTA–20% glycerol–0.2% bromophenol blue–200 μg of soybean trypsin inhibitor per ml–400 U of aprotinin per ml–10 mM β-aminocaproic acid–2 mM benzamidine–4 mM phenylmethylsulfonyl fluoride. Where indicated, 50 mM DTT was added for the reduction of proteins. Samples were boiled for 4 min before being loaded onto SDS-polyacrylamide gels.

Transfection. Transfections were performed as described previously (7, 41), using DEAE-dextran and chloroquine. The gene encoding NS28 (a kind gift from A. R. Bellamy) was inserted into the eucaryotic expression vector pSVL (Pharmacia) as described previously (7). Cos-7 cells were grown in 100-mm-diameter dishes to 80% confluency in DMEM supplemented with 5% fetal bovine serum, 5% calf serum, 2 mM L-glutamine, 100 U of penicillin per ml, and 100 μg of streptomycin per ml. Cells were rinsed in Tris-buffered saline (1.75 ml per dish) before transfection. DNA at a concentration of 20 μg/ml was added, followed by addition of 50 μg of DEAE-dextran (2×10^6 Da; Pharmacia) per ml. After 1.5 h at 37°C, the Tris-buffered saline was removed, growth medium containing 100 μM chloroquine (5.0 ml per dish; Sigma) was added, and the cells were incubated at 37°C for 3 h. After removal of the chloroquine, growth medium (10 ml per dish) was added and the cells were incubated at 37°C for 40 h. During radiolabeling, the cells were preincubated at 37°C in methionine-deficient growth medium for 10 min and then labeled for 4 h in 1 ml of methionine-deficient growth medium to which 150 μCi of L-[^{35}S]methionine was added. The cell monolayers were rinsed with ice-cold 1× PBS, and the cells were harvested in ice-cold 1× PBS by using a rubber policeman.

Gel electrophoresis and densitometry. Samples were analyzed on either 11 or 8% SDS-polyacrylamide gels (30), using a constant current power source. Gels were fixed, fluorographed in Amplify (Amersham), dried, and then fluorographed at −70°C, using Kodak SB 5 film. Densitometry of autoradiograms was performed by using an LKB 2222-010 Ultrascan XL laser densitometer (LKB Produkter AB, Sweden) in the linear range. Lower- and higher-exposed autoradiograms were used to confirm peaks.

RESULTS

Sedimentation analysis of virus-encoded proteins in infected cell lysates. To study the oligomeric state of VP7 and NS28 in SA11-infected Ma104 cells, Triton X-100-solubilized cell lysates were subjected to rate zonal sedimentation on sucrose gradients. The gradients were fractionated and analyzed by reducing and nonreducing SDS-PAGE. The lateral position (i.e., sucrose gradient fraction number) of proteins on the reducing gels indicates oligomeric state. The apparent molecular weight of the proteins corresponds to the monomeric state not the oligomeric state.

VP7, 39 kDa (Fig. 1, +DTT), sedimented with a peak at fraction 36 corresponding to an $s_{20,w}$ value of 5.0S, higher than the expected $s_{20,w}$ of 3.0S possibly because of oligomerization of VP7. Although the VP7 zone peaked in fraction 36, more rapidly sedimenting forms trailed down the gradient, indicating a range of higher forms of oligomerization. In nonreducing gels (Fig. 1, −DTT), VP7, appearing as 37 kDa, once again peaked in fraction 36, with faster-sedimenting species also present. It is concluded that VP7 is able to form higher-order complexes, allowing it to sediment more quickly in the gradient. Such multimeric forms of VP7 were not detected on the SDS-polyacrylamide gels, showing that VP7 oligomers were unstable in the SDS-gel analysis conditions.

NS28 had a sedimentation peak at fraction 32 on reducing (Fig. 1, +DTT) and nonreducing (−DTT) gels corresponding to a sedimentation rate of 7.5S. Such a sedimentation rate is not consistent with monomeric NS28. Similar to the case with VP7, faster-migrating forms were present. A 56-kDa protein, possibly an NS28 dimer, had a sedimentation peak also in fraction 32 (Fig. 1). Under reducing conditions, the comparative intensities of the 28-kDa band and the 56-kDa band were reversed (Fig. 1). This result is consistent with the latter band being an NS28 dimer and contributing its intensity to the monomeric band. Not all of the labeled protein at 56 kDa was eliminated by reduction (Fig. 1). This band may represent NS53, which was masked under nonreducing conditions by the presence of the dimer; alternatively, this band may represent a form of the NS28 dimer that is resistant to reduction. When the membrane proteins were solubilized with 1% DOC and more rigorous gel solubilization conditions were used (25), there was a reduction of the 56-kDa protein with the concomitant appearance of monomeric NS28 (data not shown). From these results, we conclude that the 56-kDa protein seen under these conditions was an NS28 homodimer, probably a relatively stable intermediate of the bulk tetrameric form sedimenting at 7.5S (see below).

The behavior of VP6 (45 kDa) also deserves comment, since it appeared prominently under reducing conditions in the faster-sedimenting fractions (Fig. 1, +DTT). This sedimentation pattern of VP6 is characteristic of higher-order structures of trimers, hexamers, and larger oligomers (22, 46). Under nonreducing conditions (Fig. 1, −DTT) less VP6 was seen, presumably because of the inability of the high-molecular-weight complexes of VP6 to enter the resolving gel.

Immunoprecipitation of NS28 oligomers. To provide further evidence that specific gradient fractions contained oligomers of NS28, Triton X-100-solubilized lysates sedimented on sucrose gradients were immunoprecipitated under denaturing conditions with an antibody made against a NS28–β-galactosidase fusion protein. Half of each sample was treated with endo H and analyzed by nonreducing

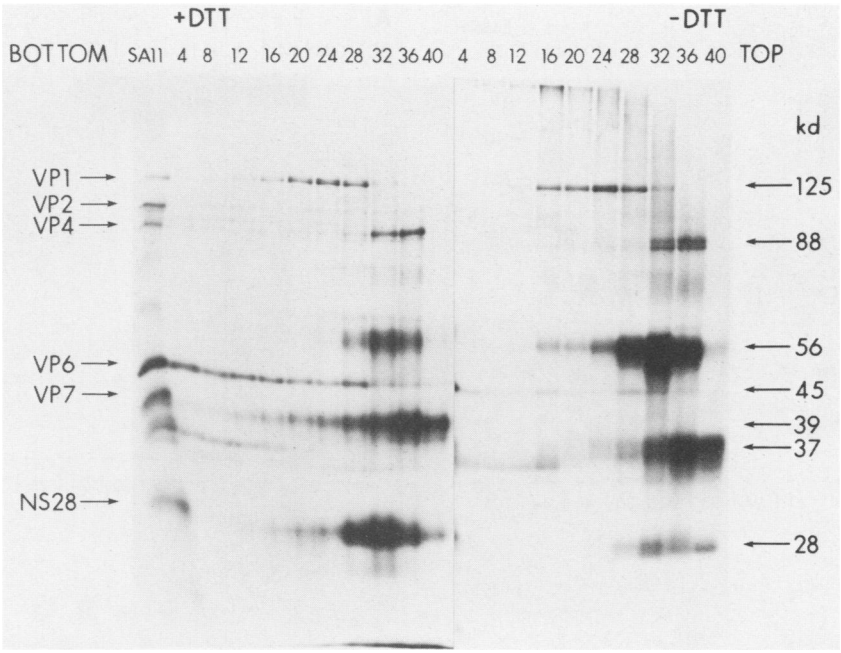

FIG. 1. Presence of rotavirus ER glycoproteins oligomers detected by sucrose gradient sedimentation. Triton X-100-solubilized infected cell lysate was fractionated on a 5 to 20% sucrose gradient for $\omega^2 t$ equal to 0.9×10^{12} rads^2/s (maximum $s_{20,w}$ of 24). Fractions in groups of four were pooled, and 1/10 of each subsequent fraction was analyzed by reducing (+DTT) and nonreducing (−DTT) 11% SDS—PAGE. Fraction number corresponds to the last pooled fraction (i.e., lane 4 is fractions 1 through 4). Fraction 4 is the bottom of the gradient, and fraction 40 is the top. Molecular sizes correspond to VP1 (125 kDa [kd]), VP4 (88 kDa), NS28 dimer (56 kDa), VP6 (45 kDa), VP7 (39 and 37 kDa), and NS28 monomer (28 kDa). Standards sedimented as follows: catalase (11.3S)-fraction 24, yeast alcohol dehydrogenase (7.6S)-fraction 32, bovine serum albumin (5.15)-fraction 36, and carbonic anhydrase (3.06S)-fraction 40. Exposure was for 5 days on Kodak SB-5 X-ray film.

SDS-PAGE. To enhance the appearance of the minor bands, the gel was overexposed (Fig. 2A). The NS28 monomer form of 28 kDa peaked in fractions 36 to 40 (2.3S to 3.2S). The NS28 dimer peaked at fractions 29 to 32 (4.2S to 5.2S), as measured by densitometry, although it was seen abundantly throughout the gradient. This was presumably due to dissociation of unstable higher-molecular-weight oligomers into stable dimers. Tetrameric NS28 (6.2S to 8.2S) peaked around fractions 12 to 24, as measured by densitometry. All of the immunoreactive forms were sensitive to endo H, indicative of the presence of high-mannose oligosaccharide found on ER-resident glycoproteins. It is known that both of the potential N-linked glycosylation sites of NS28 are utilized, resulting in an increase of its apparent molecular size by 8 kDa, (10, 16, 34). The NS28 dimer was reduced by about 12 to 16 kDa by the release of the high-mannose form of carbohydrate, consistent with the expected four N-linked glycosylation sites present in the dimer (Fig. 2A). This was confirmed by an endo H titration on the dimer, where two to three intermediate forms of deglycosylated dimer were observed (data not shown). An endo H-sensitive 85-kDa protein (Fig. 2A) may be a trimeric breakdown intermediate of the tetramer, because the bulk of NS28 consists of predominantly a 110-kDa tetramer. Hexamers and other high-molecular-weight complexes also were present but were unstable and dissociated into unstable trimers, stable dimers, and monomers under SDS-PAGE conditions.

Immunoprecipitation of VP7 oligomers. To further characterize VP7 oligomers, sucrose gradients fractions were immunoprecipitated with antibody L56, which recognizes the ER-associated form of VP7 under denaturing conditions (26). This antibody precipitated the endo H-sensitive VP7 monomer of 39 kDa throughout the sucrose gradient (Fig. 2B) with quantitative peaks, as measured by densitometry, in fractions 28 to 32 (4.2S to 5.2S), corresponding to the dimeric form, and in fraction 16 (8.2S), corresponding to a tetrameric form. We thus reinforce the conclusion from Fig. 1 that VP7 was able to form oligomers which sediment further through the sucrose gradient but were unstable in subsequent analysis by SDS-PAGE.

To determine the location of virus in the gradients, antibody 72A4, which recognizes only the virus associated form of VP7 (26) under nondenaturing conditions, was used to immunoprecipitate sucrose gradient fractions. The majority of the virus pelleted during centrifugation (Fig. 2C), with a minor amount found near the bottom of the gradient (fractions 4 to 12). In other gradient fractions, the absence of the characteristic stoichiometries of the viral structural proteins VP1 (125 kDa), VP2 (94 kDa), VP4 (88 kDa), VP6, and VP7 showed the virus was not present in these fractions. Thus, the bulk of VP7, detected with antibody L56 sedimenting beyond the monomeric peak, at fractions 28 to 32 and fraction 16 (4.7S and 8.2S; Fig. 2), was not associated with double-shelled virus. It is not known whether antibody L56 is able to detect the presence of VP7 on the membrane-enveloped double-shelled viral intermediate found in the ER lumen. However, from its expected density, the membrane-bound viral particle should pellet during centrifugation as does mature virus.

Cross-linking of NS28 to form dimers and tetramers. The sucrose gradient sedimentation analysis described above indicated the presence of oligomeric forms of NS28 and VP7. However, for the most part, such oligomers were apparently unstable and were not detected as oligomers by SDS-PAGE.

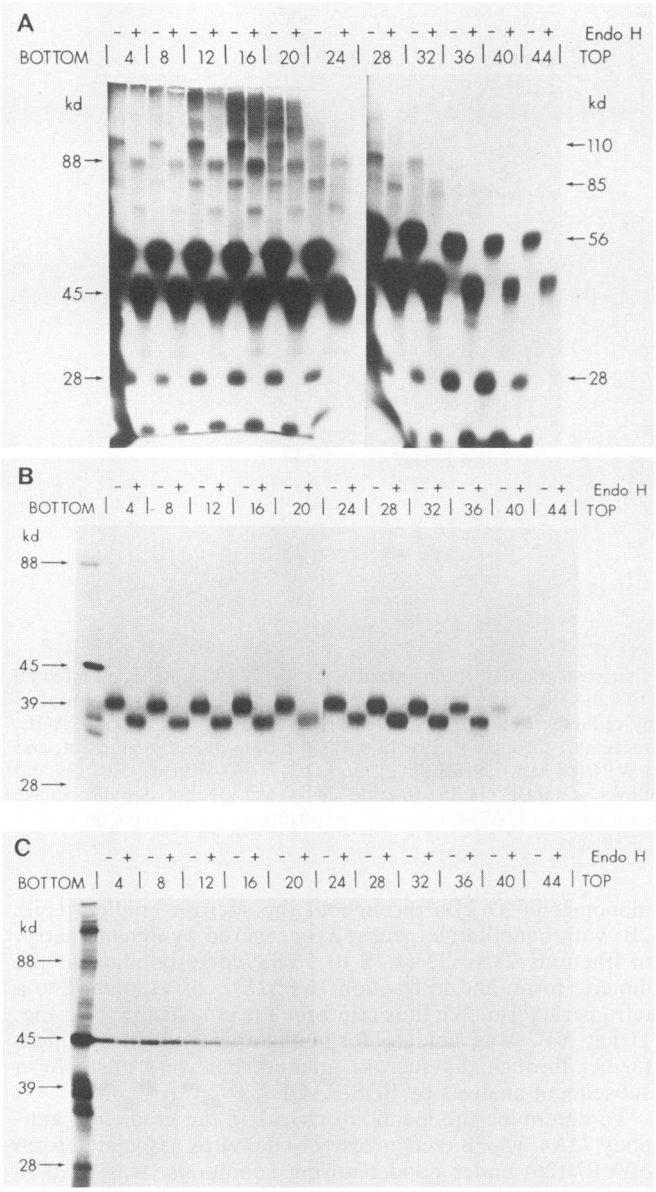

FIG. 2. Presence of faster-migrating species of VP7 and NS28 in sucrose gradients detected immunologically. Immunoprecipitation was performed on the Triton X-100-solubilized infected cell lysate run on a 5 to 20% sucrose gradient for $\omega^2 t$ equal to 1.9×10^{12} rads^2/s (maximum $s_{20,w}$ of 12) with antibodies that recognize the rotavirus glycoproteins (see Materials and Methods). (A) Anti-NS28 and (B) anti-VP7 antibody L56, both under denaturing conditions; (C) anti-VP7 antibody 72A4 under nondenaturing conditions. Half of each sample was treated with endo H and analyzed by nonreducing (A) and reducing (B and C) 11% SDS-PAGE. Molecular sizes on the right side (in kilodaltons [kd]) correspond to NS28 oligomers detected. Standards sedimented as follows: catalase-fraction 4, yeast alcohol dehydrogenase-fraction 20, bovine serum albumin-fraction 28, ovalbumin (3.7S)-fraction 36, and cytochrome *c* (1.9S)-fraction 44. Because of the number of samples, the photograph is a composite of two gels run simultaneously. Exposure was for 20 days except for panel B, which was exposed for 10 days.

To directly demonstrate these oligomers by electrophoresis, we used the cleavable homobifunctional cross-linking reagent DSP (32). DSP was added to Triton X-100-solubilized infected cell lysates before sucrose gradient centrifugation.

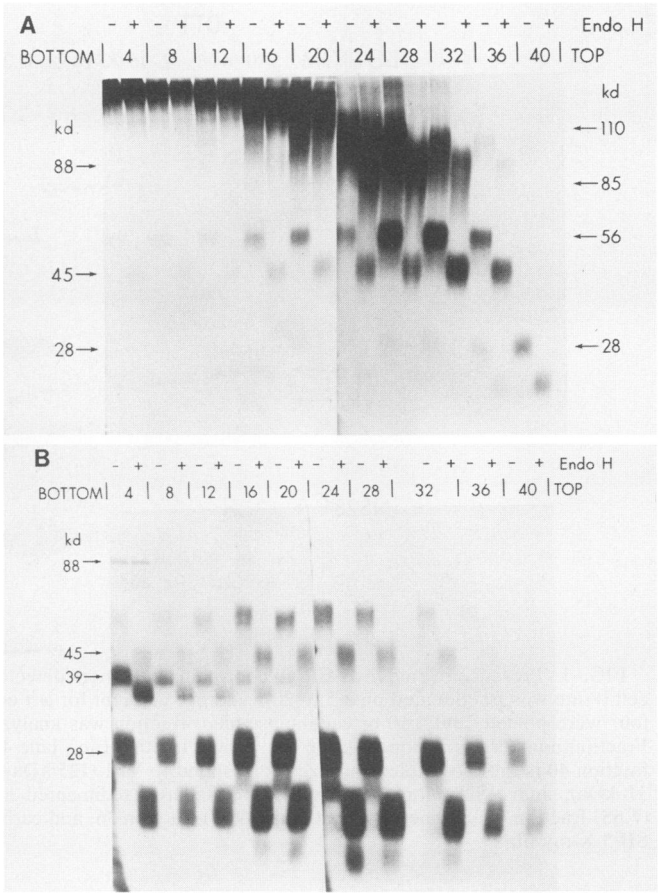

FIG. 3. Cross-linking of NS28, demonstrating that the major NS28 oligomer is tetrameric. Triton X-100-solubilized infected cell lysate was cross-linked with DSP and fractionated on a sucrose gradient run to $\omega^2 t$ equal to 1.3×10^{12} rads^2/s (maximum $s_{20,w}$ of 17). The fractions were immunoprecipitated with anti-NS28 antibody under denaturing conditions. Half of each sample was treated with endo H and analyzed by nonreducing 8% SDS-PAGE (A) and reducing 11% SDS-PAGE (B). Standards sedimented as follows: catalase-fraction 12, hexokinase (5.8S)-fraction 24, ovalbumin-fraction 32, and cytochrome *c*-fraction 40. Exposure was for 10 days.

The sucrose gradient fractions were immunoprecipitated under denaturing conditions with the anti-VP7 and anti-NS28 antibodies, and products were analyzed by reducing and nonreducing SDS-PAGE in both the presence and absence of endo H.

The behavior of NS28 in cross-linked fractions is shown in Fig. 3A. The majority of the monomeric NS28 was found in fractions 36 to 40 (1.2S to 2.4S), with little found elsewhere. The majority of dimer was seen in fractions 28 to 32 (3.5S to 4.8S), with a minor amount in faster-sedimenting fractions, possibly as a result of un-cross-linked higher oligomeric species that dissociated upon SDS-PAGE. There was no significant amount of the 85-kDa trimer, but the 110-kDa tetramer was seen as the most abundant form of NS28 in fractions 24 to 28 (4.8S to 6.5S). There was a higher-molecular-weight species in fractions 16 to 20 (7.8S to 9.0S), possibly corresponding to hexamers. The significance of high-molecular-weight complexes seen in even faster-sedimenting fractions (4 to 16) is examined below.

Components of the oligomeric forms of NS28. To analyze the composition of the immunoprecipitated cross-linked

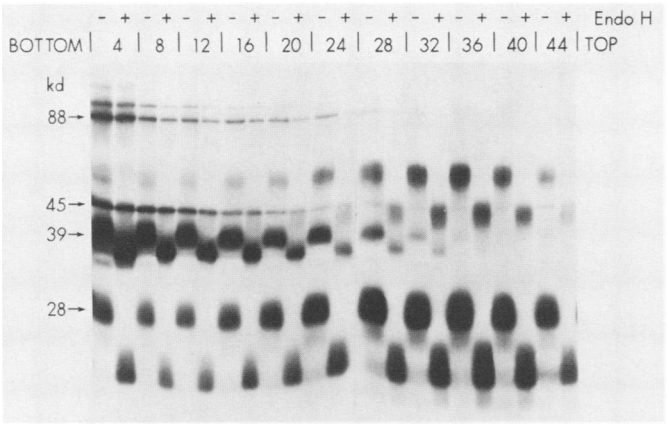

FIG. 4. Immunoprecipitation of cross-linked NS28 oligomers under nondenaturing conditions. Triton X-100-solubilized infected cell lysate was cross-linked with DSP and fractionated on a sucrose gradient that was spun to $\omega^2 t$ equal to 0.9×10^{12} rads^2/s. Fractions were immunoprecipitated under nondenaturing conditions with anti-NS28 antibody. Half of each sample was treated with endo H and analyzed by reducing 11% SDS-PAGE. Standards sedimented as in Fig. 1. Exposure was for 10 days.

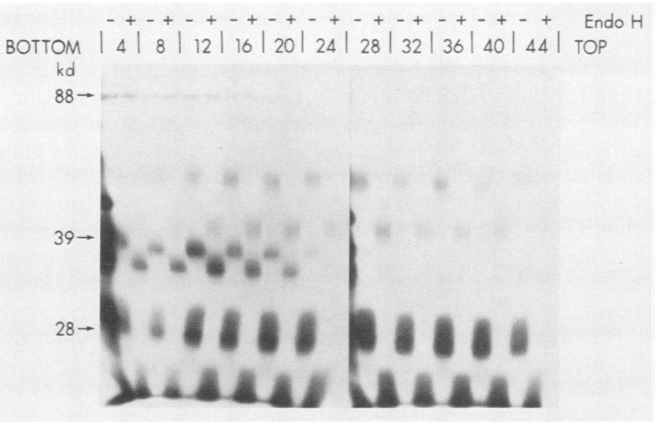

FIG. 5. Immunoprecipitation of cross-linked NS28 oligomers from sucrose gradients spun for a shorter time than for Fig. 3. Triton X-100-solubilized infected cell lysate was cross-linked with DSP and fractionated on a sucrose gradient that was spun to a $\omega^2 t$ equal to 0.6×10^{12} rads^2/s (maximum $s_{20,w}$ of 36). The fractions were immunoprecipitated with anti-NS28 antibody under denaturing conditions. Half of each sample was treated with endo H and analyzed by reducing 11% SDS-PAGE. Standards sedimented as follows: catalase-fraction 24, yeast alcohol dehydrogenase-fraction 32, bovine serum albumin-fraction 36, ovalbumin-fraction 40, and cytochrome *c*-fraction 44. Exposure was for 10 days.

species, the cross-linker was broken by thiol reduction. Reversing the cross-link demonstrated that the higher-molecular-weight forms and the faster-sedimenting dimers and tetramers were indeed oligomeric forms of NS28 (Fig. 3B). Intense bands of monomers that appeared in fractions 16 to 20 possibly originated from the high-molecular-weight hexamers. Those seen in fractions 24 to 28 originated from tetramers, and those in fractions 28 to 32 arose from dimers. The NS28 dimers that were resistant to reduction mirrored the sedimentation pattern of the monomer, although in lesser amount, indicating the probable tetrameric origin of both: Though NS28 monomers and dimers appeared in fractions 4 to 32 at different intensities, the peak in fraction 24 confirmed that the tetramer seen in Fig. 3A was the predominant form of NS28. These data, taken together with the pattern of NS28 oligomers seen in Fig. 1 and 2, argue that the predominant native form of NS28 is a tetramer.

The origin of NS28 monomers at the bottom of the gradient (fractions 4 to 16; Fig. 3B) after cross-linker reduction is more complex. The cleavage products of these complexes contained in addition to NS28 monomers and dimers, VP4 and VP7, the outer shell structural proteins of the mature rotavirus, with only minor amounts of VP6.

To eliminate the possibility that the appearance of VP7 and VP4 in this complex was due to virus, immunoprecipitation of the cross-linked material was performed under nondenaturing conditions that would preserve the virus structure. Although there was an increase in the appearance of the rotavirus structural proteins (Fig. 4), the stoichiometry of these proteins did not correspond to that of mature virus seen in fractions 4 to 12 in Fig. 2C. The inner shell structural protein, VP6, for example, was present in too small a quantity for the various subviral forms to account for the large amounts of VP4 and VP7 seen in these fractions. Thus, the appearance of the outer shell proteins, VP7 and VP4, is not due to the presence of virus in these fractions.

Another possibility to explain the presence of VP7, VP4, and NS28 in a cross-linkable complex is that there is an association of NS28, known to be an ER transmembrane protein with luminal and cytoplasmic domains (7, 11, 17, 25), with both VP7 and VP4 on their respective sides of the membrane. Shorter centrifugation times of this complex showed that the constituent proteins maintained their stoichiometries in the peak fraction (fraction 12) further up the gradient (Fig. 5). This corresponds to an $s_{20,w}$ of 16S to 20S, suggesting that a distinct heteroligomer is formed, although the oligomeric state of the proteins in these complexes remains unknown.

Orientation of the 16S to 20S heteroligomer. Semi-intact cells were used to introduce cross-linking agents into the cytoplasm while the intracellular organelles were left intact (6). Thus, the orientation of the heteroligomer of NS28, VP7,

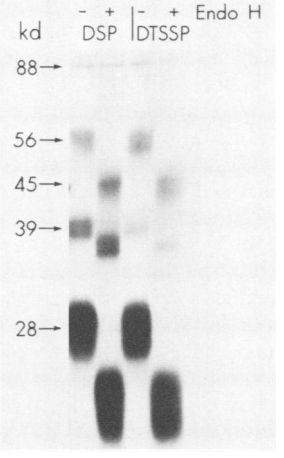

FIG. 6. Demonstration that VP7 found in the heteroligomers is in the ER lumen. Infected permeabilized cells were cross-linked with either the membrane-permeable cross-linker DSP or the membrane-impermeable crosslinker DTTSP. Triton X-100-solubilized cell lysates were immunoprecipitated with anti-NS28 antibody under denaturing conditions. Half of each sample was treated with endo H and analyzed by reducing 11% SDS-PAGE. Exposure was for 5 days.

and VP4 could be demonstrated (Fig. 6). Infected cells were permeablized, and either DSP or its water-soluble analog DTSSP was added; the preparation was then immunoprecipitated with anti-NS28 antibody under denaturing conditions. DSP, which is membrane permeable (32), was able to cross-link VP4, VP7, and NS28. The membrane-impermeable crosslinker DTSSP (48) was able to cross-link only VP4 to NS28, with a minor amount of VP7 (Fig. 6), indicating that the VP7 seen in these complexes was in fact luminally oriented in the ER. We conclude that the complex formed reflects the expected membrane disposition of VP4 (cytoplasmic), VP7 (luminal), and NS28 in infected cells.

The cross-linker does not cross-link preexisting monomers. To investigate whether the cross-linker acted nonspecifically to form oligomers of NS28 from monomers, Triton X-100-solubilized infected cell lysates were sedimented on a sucrose gradient before cross-linking, and fractions were then cross-linked with DSP, immunoprecipitated with anti-NS28 antibody under denaturing conditions, and analyzed by reducing and nonreducing SDS-PAGE. The sedimentation pattern was the same as for cross-linking before gradient analysis. NS28 seen in fractions 36 to 40 (1.5S to 2.8S) remained as a monomer, and little monomer was seen elsewhere (Fig. 7A). The NS28 dimer was seen predominantly in fractions 28 to 32 (3.5S to 4.8S), with the remainder spread throughout the gradient, probably as a result of breakdown products of higher-order oligomeric complexes. The 110-kDa tetramer was seen in fractions 12 to 24 (6.7S to 8.7S). Small amounts of the 85-kDa trimer were detected in fractions 16 to 28, as were some higher-molecular-weight complexes sedimenting further through the gradient. The majority of NS28 dimer migrated in fractions 28 to 32, and only monomeric NS28 was seen in fractions 36 to 40. Thus, the cross-linking treatment stabilized the oligomers that were already formed and did not artifactually produce oligomers from monomers. Upon cleavage of the cross-linker (Fig. 7B), the NS28 monomer and dimer were seen in all fractions. VP7 was seen as a component cross-linked in the complexes in fractions 4 to 20 as discussed above (Fig. 3B). The fact that no VP4 was seen in the complexes with VP7 may be due to a noncovalent interaction of VP4 with NS28, which cannot withstand sucrose gradient centrifugation without the prior stabilizing cross-linking reaction.

Cross-linking VP7 and immunoprecipitation. To demonstrate oligomeric forms of VP7 by SDS-PAGE, cross-linked gradient fractions were immunoprecipitated with L56 under denaturing conditions and analyzed by nonreducing and reducing SDS-PAGE (Fig. 8A). Two forms of endo H-sensitive monomeric VP7, 39 and 35 kDa, respectively, were seen in fractions 32 to 40 (2.3S to 4.2S). The two forms of cross-linked monomeric VP7 may represent two states of VP7. The form exhibiting the higher electrophoretic mobility may be intramolecularly cross-linked to form a more compact structure, and the species showing lower electrophoretic mobility may represent un-cross-linked VP7. This interpretation is reinforced by the observation that when the cross-linker was cleaved, only one form of VP7 was present (see below). Altered migration of VP7 was also seen in reducing versus nonreducing SDS-PAGE (Fig. 1). Two proteins with molecular sizes of 78 and 72 kDa were seen in fractions 28 to 32 (4.2S to 5.5S), corresponding to VP7 dimers (Fig. 8A). A protein with a molecular size of 110 kDa was seen in fractions 24 to 28 (5.5S to 6.8S), possibly a trimer, and a protein with a molecular size of 140 kDa, corresponding to a tetramer, was seen in fractions 16 to 20 (8.0S to 9.0S). There were larger species in the faster-sedimenting fractions. The predominant oligomeric form of VP7, however, was a dimer.

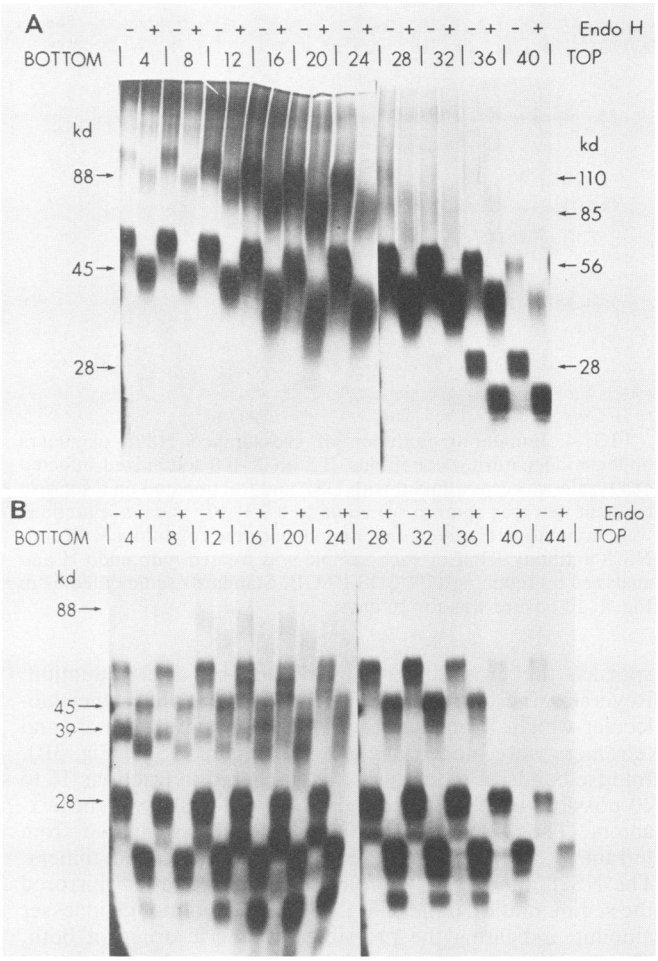

FIG. 7. Demonstration that NS28 oligomers exist as dimers, tetramers, and higher-molecular-weight complexes in distinct gradient fractions before cross-linking. Triton X-100-solubilized infected cell lysate was fractionated on a sucrose gradient spun for $\omega^2 t$ equal to 1.9×10^{12} rads^2/s, cross-linked with DSP, and immunoprecipitated with anti-NS28 antibody under denaturing conditions. Half of each sample was treated with endo H and analyzed by nonreducing 8% SDS-PAGE (A) and reducing 11% SDS-PAGE (B). Standards sedimented as in Fig. 2. Exposure was for 20 days.

Components of oligomeric VP7. When cross-linked VP7 was analyzed after cleavage of the cross-linker, only the endo H-sensitive 39-kDa monomeric VP7 was seen in all fractions throughout the gradient (Fig. 8B). It may be that heteroligomers of VP7, VP4, and NS28 were not seen in fractions 4 to 16 because unassociated homoligomers of VP7 were also present in these fractions in greater amounts than the heteroligomers, thus masking a relatively minor biosynthetic intermediate. When the unfractionated lysate, which had been cross-linked, was immunoprecipitated under denaturing conditions with antibody L56, reduced, and then run in a single lane, a small amount of NS28 was detected (data not shown), supporting this interpretation.

Cross-linking VP7 after gradient sedimentation. The same oligomeric pattern was seen when un-cross-linked Triton X-100-solubilized infected cell lysates were centrifuged on sucrose gradients and the fractions were cross-linked, immunoprecipitated with antibody L56 under denaturing con-

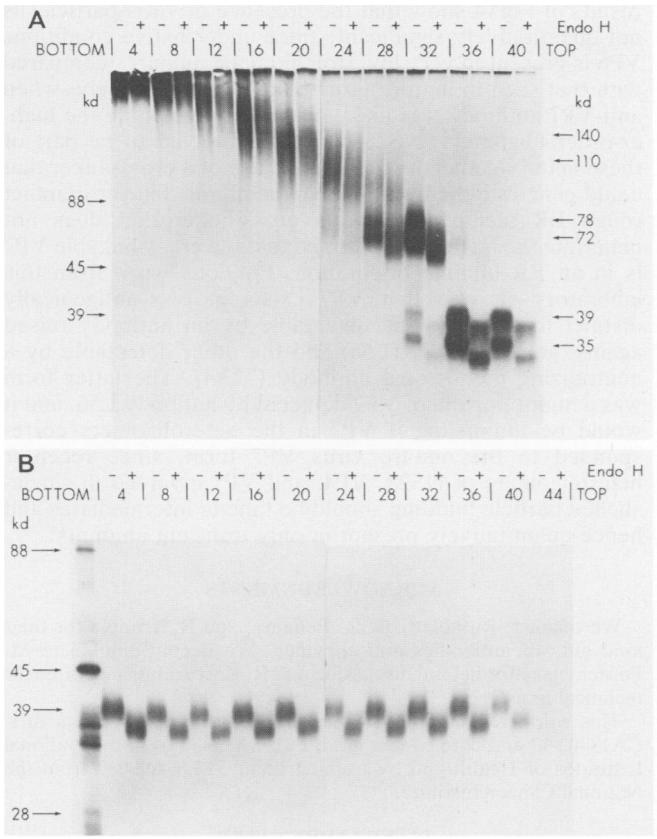

FIG. 8. Cross-linking of VP7, showing that the major oligomer is dimeric. Samples prepared as for Fig. 3 were immunoprecipitated under denaturing conditions with anti-VP7 antibody L56. Half of each sample was treated with endo H and analyzed by nonreducing 8% SDS-PAGE (A) and reducing 11% SDS-PAGE (B). Molecular sizes on the right (in kilodaltons [kd]) correspond to VP7 oligomers detected. Exposure was for 10 days.

ditions, and then analyzed by reducing and nonreducing SDS-PAGE (data not shown). It was observed that cross-linking stabilized the complexes that were formed and that they migrated to their respective positions on the sucrose gradient and did not nonspecifically cross-link neighboring monomeric VP7 molecules. The molecular weights and endo H sensitivity of these immunoreactive species suggested that the VP7 oligomers were predominantly dimers of VP7, with trimers, tetramers, and higher-order complexes of VP7 also present.

Oligomer form of NS28 in transfected cells. Cos-7 cells were transfected with Nebraska cattle diarrhea virus NS28 cDNA (5), and Triton X-100-solubilized cell lysates were cross-linked with DSP, immunoprecipitated under denaturing conditions with anti-NS28 antibody, and treated in the presence or absence of endo H. Analysis of the products by reducing and nonreducing SDS-PAGE revealed the NS28 tetramer under nonreducing conditions (Fig. 9, −DTT). Also seen was the 56-kDa dimer, with minor amounts of the monomer and higher oligomeric forms, mirroring the infected cell pattern of NS28 oligomerization. This result indicated that oligomerization of NS28 into tetramers can occur independently of other viral proteins. Reduction of the cross-linker resulted in the appearance of only NS28 monomer and dimer; no other protein was detected in the cross-linked tetramer (Fig. 9, +DTT). Unlike the case for infected

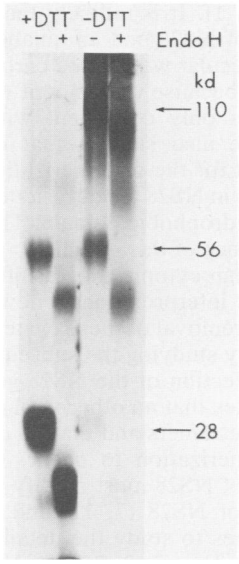

FIG. 9. Expression and cross-linking of transfected NS28 in Cos-7 cells. NS28 cDNA was transfected into Cos-7 cells and metabolically labeled. Cell lysate was cross-linked, and immunoprecipitated with anti-NS28 antibody under denaturing conditions. Half of each sample was treated with endo H and analyzed by reducing and nonreducing 11% SDS-PAGE. Exposure was for 10 days.

cells, host cellular proteins should be labeled; thus, the appearance of only NS28 monomer and dimer demonstrates that the 110-kDa protein is a homotetramer of NS28 and is the predominate form of NS28 in the cell. The level of expression of VP7 in transfected cells was inadequate to determine its oligomeric state (data not shown).

DISCUSSION

During rotavirus maturation, inner shells apparently assemble in specialized regions of the cytoplasm and then associate with the cytoplasmic face of the rough ER (1, 12, 47). The assemblage then buds into the lumen of the rough ER, acquiring a membrane in a process visually similar to the budding of membrane-enveloped viruses. Single-shelled particles appear to be precursors to mature double-shelled nonenveloped virus (2, 3, 26, 35), and the budding process takes about 15 min (26). Components of the membrane are lost by an unknown mechanism, and mature particles form, transferring VP4 and VP7 to the outer shell of the mature particles. The initial events in the budding of the single-shelled particles involve their binding to the cytoplasmic tail of the rotavirus-encoded transmembrane glycoprotein, NS28, which is thus designated the single-shelled particle receptor (2, 3, 35). The study reported here was designed to elucidate the oligomeric structure of some of the rotavirus-encoded proteins that may be involved in this assembly behavior.

We have concluded that NS28 is predominantly a tetrameric structure, although higher-order oligomers were observed. Our determination was by immunoprecipitation of cross-linked and non-cross-linked postnuclear supernatants fractionated by sucrose gradient centrifugation. A 110-kDa endo H-sensitive protein was seen under all conditions and was the predominant species when the oligomers were stabilized by cross-linking (Fig. 3A). NS28 was also able to form SDS-resistant dimers that were susceptible to reduc-

tion by DTT (Fig. 1). It is unlikely that this is a disulfide-bonded complex of NS28 and an unlabeled cellular protein with a similar molecular weight and carbohydrate content of monomeric NS28 because the amount of monomer derived from the dimer is only consistent with the dimer being homogeneous. We also suggest that disulfide bonds are responsible in part for the oligomerization of this molecule. The only cysteines in NS28 are at residues 63 and 71, located within the third hydrophobic domain. This interaction could explain the resistance of this domain to proteolytic degradation (7, 11), although cytoplasmic disulfide bonds are rarely encountered. This interpretation is now being investigated by the systematic removal of these cysteines via site-specific mutagenesis and by studying the subsequent effect on oligomerization. Transfection of the NS28 gene into Cos-7 cells clearly demonstrates that no other viral or cellular protein is associated in the tetramers and that no other viral protein is needed for oligomerization to occur. Our observation of multimeric forms of NS28 must modify the model proposed for the topology of NS28 (7, 11) and also would modify intended approaches to study the detailed nature of single-shelled particle binding (2, 3, 35) via VP6 trimers (22, 46). Clearly the nature of the exterior surface of the NS28 tetramer must be determined to more fully understand the single-shell binding process.

VP7, a membrane-associated protein, is predominantly a dimeric structure, although higher-order oligomers were seen. Two types of cross-linked monomers and dimers were seen which, upon reversal of the cross-linker, resulted in the appearance of only a single monomeric form. It is known that VP7 ultilizes intramolecular disulfide bonds, since different electrophoretic mobilities were observed under reducing and nonreducing conditions (22). The cross-linked forms seen in this study might correspond to these two forms. Thus, cross-linking of VP7 could provide a means to investigate the effect of disulfide bonding on the assembly of the outer shell in the maturation of rotavirus.

VP7 contains carbohydrate of the high-mannose type which is processed to predominantly $Man_8GlcNAc$ and $Man_6GlcNAc$ species within the ER (25). This carbohydrate processing is blocked by the energy inhibitor carbonyl cyanide *m*-chlorophenylhydrazone (25), although the ER mannosidases do not require ATP for their hydrolytic activity. This suggests that a transport event requiring energy (ATP) is necessary for VP7 to be presented as a substrate for the ER mannosidases. We are now investigating whether VP7 oligomers are necessary for this processing event to occur.

Our studies implicate the existence of cross-linkable heteroligomers consisting of VP7, NS28, and VP4. These high-molecular-weight species were found to sediment near the bottom of the sucrose gradient, and after immunoprecipitation with anti-NS28 antibody and reversal of the cross-linker, VP4, NS28, and VP7 were found to be present in near-stoichiometric amounts. This is somewhat surprising, since VP7 was localized to the ER lumen (13, 38, 39, 43) and it totally protease protected in microsomal membranes (27). VP4, on the other hand, does not contain a signal sequence (33) and is thought to have a cytoplasmic localization (25, 39). One possibility is the presence of the membrane-bound viral intermediate in these fractions, but in this case one would also expect the presence of the other viral structural proteins. Upon overexposure (Fig. 3B), a slight amount of VP6 was detected (data not shown), indicating that these fractions may contain some viral forms, including the membrane-enveloped double-shelled intermediate. However, the results of Fig. 4 show that the presence of virus particles is not quantitatively significant, since under native conditions VP6 is present in very low stoichiometic amounts compared with that seen in mature virus (Fig. 2C). Conversely, when anti-VP7 antibody was used to immunoprecipitate the higher-order oligomers, NS28 could be detected to be part of these heteroligomers. Comparative use of a cross-linker that could penetrate the hydrophobic membrane bilayer in intact rough ER membranes and a cross-linker that does not penetrate the membrane affirmed that the cross-linkable VP7 is in an ER luminal orientation. Previous work from this laboratory showed that VP7 exists in two antigenically distinct forms (26), one detectable by an antibody raised against gel band VP7 (L56) and the other detectable by a neutralizing monoclonal antibody (72A4). The latter form was a minor portion of VP7 detected by antibody L56, and it would be interesting if VP7 in the heteroligomers corresponded to the mature virus VP7 form, since receptor heteroligomers of NS28, VP4, and VP7 involved in single-shelled particle budding should be kinetic intermediates and hence quantitatively present in only transient amounts.

ACKNOWLEDGMENTS

We thank J. Rothblatt, A. R. Bellamy, and R. Trimble for their kind gifts of antibodies and enzymes. We deeply appreciate M. Poruchynsky for helpful discussion and R. Kawakami and J. Lee for technical assistance.

This work was supported by Public Health Service grants R01-CA13402-17 and core cancer grant P01-CA13330 from the National Institutes of Health and by training grant 5T32CA09060 from the National Cancer Institute.

LITERATURE CITED

1. **Altenburg, B. C., D. Y. Graham, and M. K. Estes.** 1980. Ultrastructural study of rotavirus replication in cultured cells. J. Gen. Virol. **46**:75–85.
2. **Au, K.-S., W.-K. Chan, J. W. Burns, and M. K. Estes.** 1989. Receptor activity of rotavirus nonstructural glycoprotein NS28. J. Virol. **63**:4553–4562.
3. **Au, K.-S., W.-K. Chan, and M. K. Estes.** 1989. Rotavirus morphogenesis involves an endoplasmic reticulum transmembrane glycoprotein. UCLA Symp. Mol. Cell. Biol. New Ser. **90**:257–267.
4. **Bass, D. M., E. R. Mackow, and H. B. Greenberg.** 1990. NS35 and not vp7 is the soluble rotavirus protein which binds to target cells. J. Virol. **64**:322–330.
5. **Baybutt, H. N., and M. A. McCrae.** 1984. The molecular biology of rotavirus. VII. Detailed structural analysis of gene 10 of bovine rotavirus. Virus Res. **1**:533–541.
6. **Beckers, C. J. M., D. S. Keller, and W. E. Balch.** 1987. Semi-intact cells permeable to macromolecules: use in reconstitution of protein transport from the endoplasmic reticulum to the Golgi complex. Cell **50**:523–534.
7. **Bergmann, C. C., D. Maass, M. S. Poruchynsky, P. H. Atkinson, and A. R. Bellamy.** 1989. Topology of the non-structural rotavirus receptor glycoprotein NS28 in the rough endoplasmic reticulum. EMBO J. **8**:1695–1703.
8. **Bole, D. G., L. M. Hendershot, and J. F. Kearney.** 1986. Posttranslational association of immunoglobulin heavy chain binding protein with nascent heavy chains in nonsecreting and secreting hybridomas. J. Cell Biol. **102**:1558–1566.
9. **Both, G. W., J. S. Mattick, and A. R. Bellamy.** 1983. Serotype-specific glycoprotein of simian 11 rotavirus: coding assignment and gene sequence. Proc. Natl. Acad. Sci. USA **80**:3091–3095.
10. **Both, G. W., L. J. Siegman, A. R. Bellamy, and P. H. Atkinson.** 1983. Coding assignment and nucleotide sequence of simian rotavirus SA11 gene segment 10: location of glycosylation sites suggests that the signal peptide is not cleaved. J. Virol. **48**: 335–339.
11. **Chan, W.-K., K.-S. Au, and M. K. Estes.** 1988. Topography of

the simian rotavirus nonstructural glycoprotein (NS28) in the endoplasmic reticulum membrane. Virology **164**:435–442.
12. **Chasey, D.** 1977. Different particle types in tissue culture and intestinal epithelium infected with rotavirus. J. Gen. Virol. **37**:443–451.
13. **Chasey, D.** 1980. Investigation of immunoperoixdase-labelled rotavirus in tissue culture by light and electron microscopy. J. Gen. Virol. **50**:195–200.
14. **Copeland, C. S., R. W. Doms, E. M. Bolzau, R. G. Webster, and A. Helenius.** 1986. Assembly of influenza hemagglutinin trimers and its role in intracellular transport. J. Cell Biol. **103**:1179–1191.
15. **Copeland, C. S., K.-P. Zimmer, K. R. Wagner, G. A. Healey, I. Mellman, and A. Helenius.** 1988. Folding, trimerization, and transport are sequential events in the biogenesis of influenza virus hemagglutinin. Cell **53**:197–209.
16. **Ericson, B. L., D. Y. Graham, B. B. Mason, and M. K. Estes.** 1982. Identification, synthesis, and modifications of simian rotavirus SA11 polypeptides in infected cells. J. Virol. **42**: 825–839.
17. **Ericson, B. L., D. Y. Graham, B. B. Mason, H. H. Hanssen, and M. K. Estes.** 1983. Two types of glycoprotein precursors are produced by the simian rotavirus SA11. Virology **127**:320–332.
18. **Estes, M. K., E. L. Palmer, and J. F. Obijeski.** 1983. Rotaviruses: a review. Curr. Top. Microbiol. Immunol. **105**:123–184.
19. **Fukuhara, N., O. Yoshie, S. Kitaoka, and T. Konno.** 1988. Role of VP3 in human rotavirus internalization after target cell attachment via VP7. J. Virol. **62**:2209–2218.
20. **Gething, M.-J., K. McCammon, and J. Sambrook.** 1986. Expression of wild-type and mutant forms of influenza hemagglutinin: the role of folding in intracellular transport. Cell **46**:939–950.
21. **Glass, R. I., J. Keith, O. Nakagomi, T. Nakagomi, J. Askaa, A. Z. Kapikian, R. M. Chanock, and J. Flores.** 1985. Nucleotide sequence of the structural glycoprotein VP7 gene of Nebraska calf diarrhea virus rotavirus: comparison with homologous genes from four strains of human and animal rotaviruses. Virology **141**:292–298.
22. **Gorziglia, M., C. Larrea, F. Liprandi, and J. Esparza.** 1985. Biochemical evidence for the oligomeric (possibly trimeric) structure of the major inner capsid polypeptide (45kd) of rotaviruses. J. Gen. Virol. **66**:1889–1900.
23. **Gluzman, Y.** 1981. SV-40-transformed simian cells support the replication of early SV40 mutants. Cell **23**:175–182.
24. **Holmes, I. H.** 1983. Rotaviruses, p. 359–423. *In* W. K. Joklik (ed.), The Reoviridae. Plenum Publishing Corp., New York.
25. **Kabcenell, A. K., and P. H. Atkinson.** 1985. Processing of the rough endoplasmic reticulum membrane glycoproteins of rotavirus SA11. J. Cell Biol. **101**:1270–1280.
26. **Kabcenell, A. K., M. S. Poruchynsky, A. R. Bellamy, H. B. Greenberg, and P. H. Atkinson.** 1988. Two forms of VP7 are involved in assembly of SA11 rotavirus in endoplasmic reticulum. J. Virol. **62**:2929–2941.
27. **Kalica, A. R., J. Flores, and H. B. Greenberg.** 1983. Identification of the rotaviral gene that codes for hemagglutination and protease-enhanced plaque formation. Virology **125**:194–205.
28. **Kapikian, A. Z., and R. M. Chanock.** 1985. Rotaviruses, p. 863–906. *In* B. N. Fields (ed.), Virology. Raven Press, New York.
29. **Kreis, T. E., and H. F. Lodish.** 1986. Oligomerization is essential for transport of vesicular somatitis viral glycoprotein to the cell surface. Cell **46**:929–937.
30. **Laemmli, U. K.** 1970. Cleavage of structural proteins during the assembly of the head of bacteriophage T4. Nature (London) **227**:680–685.
31. **Liu, M., P. A. Offit, and M. K. Estes.** 1988. Identification of the simian rotavirus SA11 genome segment 3 product. Virology **163**:26–32.
32. **Lomant, A. J., and G. Fairbanks.** 1976. Chemical probes of extended biological structures: synthesis and properties of the cleavable protein cross-linking reagent [^{35}S]dithiobis(succinimidyl propionate). J. Mol. Biol. **104**:243–261.
33. **Mackow, E. R., R. D. Shaw, S. M. Matsui, P. T. Vo, M.-N. Dang, and H. B. Greenberg.** 1988. The rhesus rotavirus gene encoding protein VP3: location of amino acids involved in homologous and heterologous rotavirus neutralization and identification of a putative fusion region. Proc. Natl. Acad. Sci. USA **85**:645–649.
34. **McEwen, C. R.** 1967. Tables for estimating sedimentation through linear concentration gradients of sucrose solution. Anal. Biochem. **20**:114–149.
35. **Meyer, J. C., C. C. Bergmann, and A. R. Bellamy.** 1989. Interaction of rotavirus cores with the nonstructural glycoprotein NS28. Virology **171**:98–107.
36. **Okada, Y., M. A. Richardson, N. Ikegami, A. Nomoto, and Y. Furuichi.** 1984. Nucleotide sequence of human rotavirus genome segment 10, an RNA encoding a glycosylated virus protein. J. Virol. **51**:856–859.
37. **Petrie, B. L., M. K. Estes, and D. Y. Graham.** 1983. Effects of tunicamycin on rotavirus morphogenesis and infectivity. J. Virol. **46**:270–274.
38. **Petrie, B. L., D. Y. Graham, H. Hanssen, and M. K. Estes.** 1982. Localization of rotavirus antigens in infected cells by ultrastructural immunocytochemistry. J. Gen. Virol. **63**:457–467.
39. **Petrie, B. L., H. B. Greenberg, D. Y. Graham, and M. K. Estes.** 1984. Ultrastructural localization of rotavirus antigens using colloidal gold. Virus Res. **1**:133–152.
40. **Poruchynsky, M. S., and P. H. Atkinson.** 1988. Primary sequence domains required for the retention of rotavirus VP7 in the endoplasmic reticulum. J. Cell Biol. **107**:1697–1706.
41. **Poruchynsky, M. S., C. Tyndall, G. W. Both, F. Sato, A. R. Bellamy, and P. H. Atkinson.** 1985. Deletions into an NH_2-terminal hydrophobic domain result in secretion of rotavirus VP7, a resident endoplasmic reticulum membrane glycoprotein. J. Cell Biol. **101**:2199–2209.
42. **Richardson, M. A., A. Iwamoto, N. Ikegami, A. Nomoto, and Y. Furuichi.** 1984. Nucleotide sequence of the gene encoding the serotype-specific antigen of human (Wa) rotavirus: comparison with the homologous genes from simian SA11 and UK bovine rotaviruses. J. Virol. **51**:860–862.
43. **Richardson, S. C., L. E. Mercer, S. Sonza, and I. H. Holmes.** 1986. Intracellular localization of rotavirus proteins. Arch. Virol. **88**:251–264.
44. **Rose, J. K., and J. E. Bergmann.** 1983. Altered cytoplasmic domains affect intracellular transport of the vesicular stomatitis virus glycoprotein. Cell **34**:513–524.
45. **Sabara, M., J. E. Gilchrist, G. R. Hudson, and L. A. Babiuk.** 1985. Preliminary characterization of epitopes involved in neutralization and cell attachment that is located on the major bovine rotavirus glycoprotein. J. Virol. **53**:58–66.
46. **Sabara, M., K. F. M. Ready, P. J. Frenchick, and L. A. Babiuk.** 1987. Biochemical evidence for the oligomeric arrangement of bovine nucleocapsid protein and its possible significance in the immunogenicity of this protein. J. Gen. Virol. **68**:123–133.
47. **Soler, C., C. Musalem, M. Lorono, and R. T. Espejo.** 1982. Association of viral particles and viral proteins with membranes in SA11-infected cells. J. Virol. **44**:983–992.
48. **Staros, J. V.** 1982. N-hydroxysulfosuccinimide active esters: bis(N-hydroxysulfosuccinimide) esters of the two dicarboxylic acids are hydrophilic, membrane-impermeant, protein cross-linkers. Biochemistry **21**:3950–3955.
49. **Stirazaker, S. C., and G. W. Both.** 1989. The signal peptide of the rotavirus glycoprotein VP7 is essential for its retention in the ER as an integral membrane protein. Cell **56**:741–747.
50. **Stirazaker, S. C., P. L. Whitfeld, D. L. Christie, A. R. Bellamy, and G. W. Both.** 1987. Processing of rotavirus glycoprotein VP7: implications for the retention of the protein in the endoplasmic reticulum. J. Cell Biol. **105**:2897–2903.
51. **Street, J. E., M. C. Croxson, W. F. Chadderton, and A. R. Bellamy.** 1982. Sequence diversity of human rotavirus strains investigated by Northern blot hybridization analysis. J. Virol. **43**:369–378.